Low-lying dipole strength in the $N = 28$ shell-closure nucleus ^{52}Cr

H. Pai,[1,*] J. Beller,[1] N. Benouaret,[1] J. Enders,[1] T. Hartmann,[1] O. Karg,[1] P. von Neumann-Cosel,[1] N. Pietralla,[1]
V. Yu. Ponomarev,[1] C. Romig,[1] M. Scheck,[1,2,3] L. Schnorrenberger,[1] S. Volz,[1] and M. Zweidinger[1]

[1]*Institut für Kernphysik, Technische Universität Darmstadt, D-64289 Darmstadt, Germany*
[2]*School of Engineering, University of the West of Scotland, PA1 2BE Paisley, United Kingdom*
[3]*Scottish Universities Physics Alliance (SUPA), Glasgow G12 8QQ, United Kingdom*

The low-lying dipole strength of the $N = 28$ closed-shell nucleus ^{52}Cr was studied with nuclear resonance fluorescence up to 9.9 MeV, using bremsstrahlung at the superconducting Darmstadt linear electron accelerator S-DALINAC. Twenty-eight spin-1 states were observed between 5.0 and 9.5 MeV excitation energy, 14 of which for the first time. Both electric dipole excitations ($E1$, around 8 MeV) and magnetic dipole excitations ($M1$, around 9 MeV) were detected. Microscopic calculations within the quasiparticle-phonon nuclear model were performed and show good agreement with experimental results. The structure of $E1$ and $M1$ excitations, respectively, is discussed.

I. INTRODUCTION

Low-lying electric and magnetic dipole strengths ($E1$ and $M1$, respectively) of atomic nuclei has drawn considerable attention in recent years [1–4]. The concentration of $E1$ strength below or in the vicinity of the particle separation energy is usually denoted as pygmy dipole resonance (PDR), whose structure is currently under debate [5–7]. The PDR is commonly assumed (macroscopic picture) to result from oscillations of excess neutrons against an isospin saturated $N \approx Z$ core. This behavior is also expected from microscopic model calculations [8,9].

Although a concentration of low-energy $E1$ strength has been observed experimentally in both stable and unstable nuclei at shell closures, for example, for the O [10,11], Ca [12–14], Ni [2,15–17], Sn [18–22], and Pb isotopes [9,23–26] as well as for the $N = 50$ [27–29] and $N = 82$ isotones [30–34], there are considerably fewer recent data on $N = 28$ isotones [35–38]. While in stable $N \approx Z$ nuclei up to ^{40}Ca the PDR is not significantly developed, in ^{48}Ca ($N = 28$), the interpretation of the low-energy $E1$ strength as PDR is under debate [39,40]. In stable $A > 50$ Ni isotopes the PDR is substantially developed already [2,15–17]. Apparently, the PDR starts to form near mass number $A \approx 50$. Experimental information on the $N = 28$ isotone ^{52}Cr may help to clarify the situation. In addition to $E1$ strength, stable fp-shell nuclei exhibit spin-flip $M1$ resonances [4,16], mainly from $f_{7/2} \rightarrow f_{5/2}$ orbitals, for both protons and neutrons.

In the present work, real photon scattering (nuclear resonance fluorescence (NRF); see Refs. [41–43]) of ^{52}Cr was studied up to 9.9 MeV in order to investigate low-lying dipole strength ($E1$ and $M1$) in the fp-shell region with improved sensitivity compared to previous work [35,36,44]. Results of the electric quadrupole ($E2$) strength distribution from the present experiment are published elsewhere [45].

II. EXPERIMENTAL METHOD AND DATA ANALYSIS

The NRF experiment was performed at the superconducting Darmstadt electron linear accelerator S-DALINAC [46] using unpolarized bremsstrahlung with end-point energies of 8.0(1) and 9.9(1) MeV, respectively. The measurements with 8.0(1) MeV bremsstrahlung were carried out to identify transitions via intermediate states. The setup is described in detail in Ref. [47]. Bremsstrahlung was produced by stopping completely the intense electron beam from the S-DALINAC's injector in a thick copper radiator target. Scattered γ rays were detected by two high-purity germanium (HPGe) detectors with 100% efficiency relative to a standard 3×3 in^2 NaI detector at 90° and 130° with respect to the incident beam. The detectors were surrounded by lead and bismuth germanate Compton suppression shields. The first measurement was performed with 996.4(5) mg of an isotopically enriched ^{52}Cr target (99.8% enriched) using an end-point energy of $E_0 = 9.9(1)$ MeV and average beam currents of about 45 μA. In this measurement data were taken for 62 h. For energy and photon-flux calibrations 1004.1(5) mg of natural boron were used that were irradiated simultaneously. The efficiency of the two HPGe detectors was determined with a ^{56}Co source up to about 3500 keV energy. For higher photon energies the γ-ray detection efficiencies were extracted from a simulation using the GEANT4 toolkit [48]. The second measurement was performed with 2954(1) mg of natural chromium (natural abundance of ^{52}Cr is 83.789%) at $E_0 = 8.0(1)$ MeV end-point energy and average beam currents of about 42 μA. In this measurement data were taken for 23 h. Photon scattering spectra of the ^{52}Cr(γ, γ') reaction between 3500 and 10 000 keV for the detector at 130°, measured at $E_0 = 9.9(1)$ MeV, are shown in Figs. 1(a), 1(b), and 1(c). In the following, transitions corresponding to direct decays to the ground state are called elastic transitions and those decaying via intermediate states are referred to as inelastic transitions.

In NRF measurements the excitation mechanism is purely electromagnetic, and intrinsic properties like spin, parity, and transition probabilities can be determined from the measured quantities (angular distribution, polarization asymmetries,

———————
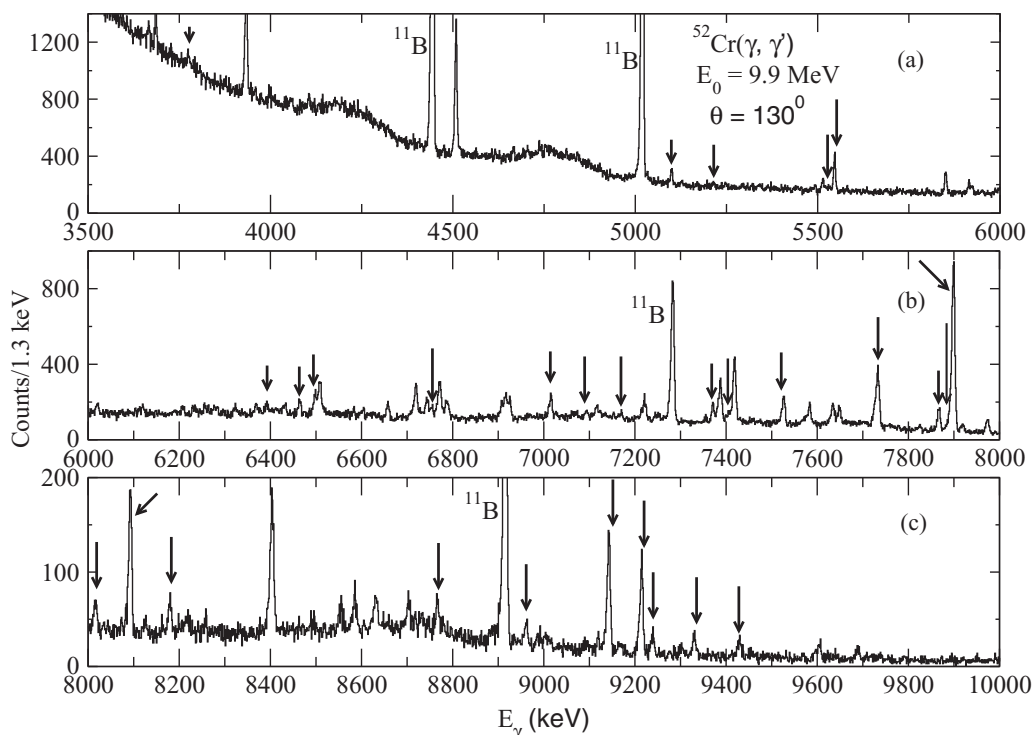*hari.vecc@gmail.com, hpai@ikp.tu-darmstadt.de

FIG. 1. Photon scattering spectra of the ^{52}Cr(γ, γ') reaction between 3500 and 10 000 keV for the 130° detector, measured at $E_0 = 9.9$ MeV. Ground-state transitions of ^{52}Cr are indicated by arrows, and unmarked peaks correspond to inelastic transitions or escape peaks, or result from background radiation.

γ-ray energy, and intensity [41–43]) in a model-independent way. For details of the analysis as well as for the basic relations between the detected number of events and energy-integrated cross sections ($I_{i,0}$), transition widths, as well as $E1$ and $M1$ transition strengths, we refer the reader to the reviews by Metzger [43] and Kneissl and co-workers [41,42].

Because not all parity quantum numbers of excited $J = 1$ states in ^{52}Cr are known, the reduced transition width into the ground state $g\Gamma_0^{\text{red}} = g\Gamma_0/E_\gamma^3$ is given as an alternative to $B(M1)$ and $B(E1)$ values, being proportional to these values. Here, $g = 3$ denotes the statistical factor of dipole excitations from the $J^\pi = 0^+$ ground state, and the partial decay width into the ground state is indicated by Γ_0 in addition to the γ energy E_γ.

III. RESULTS AND DISCUSSION

The experimental results are summarized in Table I. Sixteen of these excited states of ^{52}Cr are already known from various earlier experiments [35–37,49,50]. However, the present experiment is more sensitive. Fourteen new states were identified in the present experiment and uncertainties for cross sections were reduced in many cases. Previously observed levels at 5213.7 keV from ^{52}Cr$(p, p')^{52}$Cr (see Refs. [50,51]) and at 6389.9 keV from ^{51}V$(^3$He, $d)^{52}$Cr and ^{51}V$(p, \gamma)^{52}$Cr (see Refs. [50,52,53]) were assigned a total angular momentum $J = 1$ from the angular distribution in the present experiment. Other known levels that have mainly been identified from the ^{52}Cr(e, e') [49] and ^{52}Cr(γ, γ') [35–37] experiments are also observed in the present work, and J^π

assignments were done. An angular momentum of $J = 1$ was found in this work for the 6495.5-keV state where a previous ^{52}Cr(γ, γ') [37] experiment had proposed $J = 2$. Definite parity quantum numbers of the 7524.1-, 7731.9-, 7897.4-, 9140.3-, and 9211.9-keV states were adopted from earlier NRF experiments with polarized bremsstrahlung [36]. For the $J = 1$ levels at 7166.2, 7865.1, 9327.0, and 9429.0 keV, positive parity was adopted, because these excitations were previously observed in a backward-angle low momentum-transfer electron scattering experiment [49]. The deduced $M1$ strengths from the present experiment are in general agreement with the (e, e') data from Ref. [49] with a few exceptions where the values from electron scattering exceed the NRF result at a two- to three-standard-deviation level. This may arise due to weak unobserved decay branches to excited states. While the high sensitivity of the (e, e') data indicates that attributing electric character to at least the stronger dipole excitations with unknown transition character is likely, we refrained from making a firm assignment to the data of Table I because an unambiguous experimental confirmation of the parities for the related $J = 1$ states is still lacking. The 6462.0-keV γ ray could be an inelastic transition depopulating the 7897.4-keV level. However, because this transition is also observed in the measurement with 8.0(1) MeV end-point energy, we consider it to be elastic.

Figure 2(a) shows the experimental results, displaying the reduced transition widths proportional to $B(M1)$ or $B(E1)$ values into the ground state for all observed dipole excitations. Magnetic dipole excitations are indicated in red, $E1$ strength is shown in green, and blue bars indicate dipole excitations

TABLE I. Transitions observed in the ^{52}Cr(γ, γ') reaction with an end-point energy of 9.9 MeV. Experimental uncertainties of the excitation energies are less than 0.5 keV.

E_x (keV)	E_γ (keV)	$\frac{W(90°)}{W(130°)}$	J^π	$I_{i,0}$ (eV b)	Γ_0 (eV)	$\frac{\Gamma_i}{\Gamma_0}$ [a]	$B(M1)\uparrow$ (μ_N^2)	$B(M1)\uparrow$[b] (μ_N^2)	$B(E1)\uparrow$ ($10^{-3}\,e^2\mathrm{fm}^2$)	$B(E1)\uparrow$[b] ($10^{-3}\,e^2\mathrm{fm}^2$)	Γ_0^{red} (meV/MeV^3)
1433.9	1433.9	1.05(12)	2+[c]	<60.6(37)[d]							
3771.5	3771.4	1.07(29)	2+[c]	<7.2(9)[d]							
5098.6	5098.3	0.54(11)	1±	11.2(18)	0.045(10)	0.79(22)	0.089(21)	0.085(13)[c]	0.98(23)	0.94(14)[c]	0.34(8)
	3664.5										
5213.7	5213.4	1.14(50)	1±	5.4(12)	0.013(3)		0.023(6)		0.259(60)		0.09(2)
5526.0	5525.7	1.13(36)	1±	5.9(10)	0.016(3)		0.024(5)		0.267(51)		0.09(2)
5544.7	5544.4	0.81(10)	1±	41.9(25)	0.112(7)		0.171(11)	0.19(4)[c]	1.88(12)	2.1(4)[c]	0.66(4)
6389.9	6389.5	1.09(22)	1±	19.5(19)	0.069(7)		0.069(7)		0.762(77)		0.27(3)
6462.4	6462.0	0.70(14)	1±	20.3(20)	0.074(7)		0.071(7)		0.784(78)		0.27(3)
6495.5	6495.1	0.72(11)	1±	35.6(25)	0.131(9)		0.124(9)		1.367(96)		0.48(3)
6752.0	6751.5	0.69(15)	1±	22.3(24)	0.089(10)		0.075(9)		0.824(92)		0.29(3)
7014.1	7013.6	0.71(11)	1±	39.5(44)	0.210(30)	0.24(6)	0.158(23)		1.74(25)		0.61(9)
	5580.5										
7090.8	7090.3	0.72(31)	1±	14.1(25)	0.062(11)		0.045(8)		0.496(88)		0.17(3)
7166.2	7165.7	0.68(27)	1+[f]	12.0(24)	0.054(11)		0.038(8)	0.121(72)[f]			0.15(3)
7368.8	7368.2	0.88(14)	1±	48.4(38)	0.229(18)		0.148(12)		1.64(13)		0.57(5)
7403.2	7402.6	0.62(21)	1±	22.5(32)	0.107(15)		0.069(10)		0.76(11)		0.26(4)
7524.1	7523.5	0.52(8)	1+[e]	81.1(56)	0.400(28)		0.243(18)	0.221(37)[f]			0.94(6)
7731.9	7731.3	0.57(8)	1−[e]	185(12)	0.960(64)				5.96(40)		2.08(14)
7865.1	7864.5	0.70(9)	1+[f]	80.9(51)	0.435(27)		0.232(15)	0.293(31)[f]			0.90(6)
7889.0	7888.4	0.58(11)	1±	88.6(83)	0.480(45)		0.253(24)		2.80(26)		0.98(9)
7897.4	7896.8	0.76(8)	1−[e]	623(32)	3.38(17)				19.7(10)		6.87(35)
8015.3	8014.6	0.83(18)	1±	30.2(50)	0.260(59)	0.54(16)	0.131(30)		1.45(33)		0.51(11)
	6580.9										
8091.3	8090.6	0.80(10)	1±	128.8(78)	0.734(44)		0.359(22)		3.97(24)		1.39(8)
8179.2	8178.5	0.74(20)	1±	36.3(58)	0.90(18)	3.26(50)	0.427(88)		4.72(98)		1.65(34)
	6740.8										
8765.9	8765.1	0.95(16)	1±	66.0(56)	0.441(37)		0.170(15)		1.88(17)		0.66(6)
8958.4	8957.6	0.49(15)	1±	33.3(52)	0.233(36)		0.084(13)		0.93(15)		0.32(5)
9140.3	9139.4	0.82(10)	1+[e]	364(21)	2.65(15)		0.898(53)	1.118(59)[f]			3.47(20)
9211.9	9211.0	0.63(8)	1+[e]	286(19)	2.11(14)		0.700(47)	0.879(50)[f]			2.70(17)
9236.6	9235.7	0.53(12)	1±	67.8(74)	0.503(55)		0.166(18)		1.83(20)		0.64(7)
9327.0	9326.1	0.55(12)	1+[f]	99(11)	0.746(80)		0.238(26)	0.235(32)[f]			0.92(10)
9429.0	9428.1	0.51(12)	1+[f]	123(15)	0.95(11)		0.295(35)	0.339(50)[f]			1.14(13)

[a]Branching ratio.
[b]From Ref. [50] compiled from primary literature indicated by footnotes.
[c]From Ref. [37].
[d]Due to feeding.
[e]NRF experiments with polarized bremsstrahlung [36].
[f]From ^{52}Cr(e, e') experiment [49].

with unknown polarity. The total strength of dipole excitations with firmly assigned radiation character exceeds the strength of unassigned character by a factor of 1.9.

Calculations within the microscopic quasiparticle-phonon nuclear model (QPM [18,54]) were performed using a basis which includes one-, two-, and three-phonon configurations to interpret the dipole strength distributions of ^{52}Cr in a microscopic way. Figure 2(b) displays the QPM predictions for magnetic (red) and electric (green) dipole strength along with the experimental detection limit of the present experiment (dotted line, $\Gamma_0/\Gamma = 1$). The $B(M1)$ values were calculated with effective g factors $g_s^{\mathrm{eff}} = 0.6 g_s^{\mathrm{free}}$. Quenching factors are determined by requiring optimum agreement with the data,

and that the corresponding factor in the QPM is 0.6, while shell-model calculations for the $N = 28$ [55,56] isotones find a factor 0.75.

The QPM results agree well with the experimental findings. In these calculations, the main one-phonon components of the strongest 1^- state are located below 10 MeV and do not belong to the giant dipole resonance. Taking the strongest $E1$ excitation as an example, the excitation energy is about 400 keV lower than predicted, and the predicted strength of $18.3 \times 10^{-3}\,e^2\mathrm{fm}^2$ almost agrees within experimental errors with the measured value of $19.7(10) \times 10^{-3}\,e^2\mathrm{fm}^2$. Energy and strength of the strongest $E1$ excitations also agree with findings in neighboring nuclei [2,16], including the fact that the
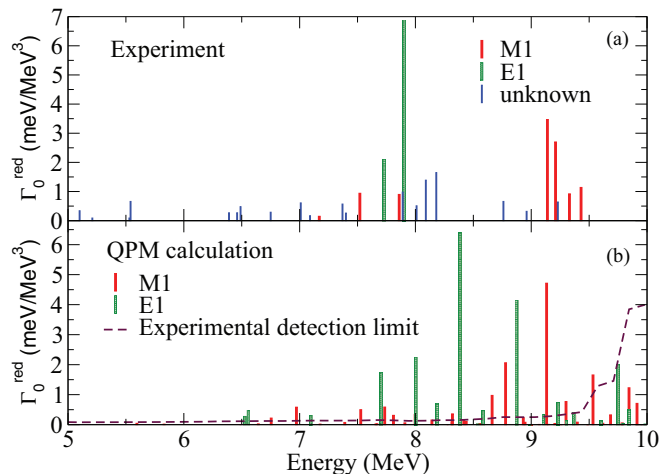
FIG. 2. (Color online) (a) The experimental reduced transition widths proportional to $B(M1)$ or $B(E1)$ values into the ground state for all observed dipole excitations. (b) Theoretical $M1$ and $E1$ strength distributions in terms of reduced transition width obtained from QPM calculations along with the experimental detection limit of the present experiment.

Thomas-Reiche-Kuhn (TRK) [57] isovector $E1$ sum rule is exhausted to less than 0.3% by this low-lying strength. Assuming electric character for the excitations at 7.37, 7.89, 8.02, 8.09, and 8.18 MeV in addition to the two known unambiguous $E1$ excitations, the TRK sum rule exhaustion amounts to $\approx 0.15\%$. This value is smaller but close to those observed for the PDR in the slightly heavier Fe and Ni isotopes [16].

Spin-$M1$ strength is well known to exist around 9 MeV excitation energy in the $N = 28$ isotones. In addition to high-resolution electron scattering data of Refs. [49,58], theoretical analyses have been shown to reproduce the measured values well. In addition to the QPM calculations presented here, a good account of the $M1$ strength distribution including an

appropriate description of the fragmentation is also obtained within the shell model [55,56]. The present data show an accumulation of $M1$ strength (for stronger excited $J^{\pi} = 1^{+}$ levels) near 9 MeV [see Fig. 2(a)] excitation energy, in agreement with the findings from electron scattering and previous photon scattering work.

This observation is also corroborated by the microscopic QPM calculations [see Fig. 2(b)]. Strong $M1$ transitions appear near 9 MeV excitation energy due to the isovector $f_{7/2} \rightarrow f_{5/2}$ spin-flip $M1$ resonance, while weaker transitions appear near 8 MeV excitation energy corresponding to the isoscalar $f_{7/2} \rightarrow f_{5/2}$ spin-flip $M1$ strength.

IV. SUMMARY AND OUTLOOK

An NRF experiment on the semimagic ^{52}Cr nucleus was performed to study its low-lying dipole strength up to 9.9 MeV. Fourteen new transitions were identified in the present experiment. The observed dipole strengths agree with microscopic QPM calculations. The occurrence of electric dipole strength in this pygmy-dipole-resonance region and spin-$M1$ excitations with comparable energy suggests the need for determining the excited states' parities through polarized photon scattering of Compton polarimetry if a more quantitative understanding would be aimed for. Further experiments in the A $\approx$ 50 mass region may provide additional information on the onset of the PDR in atomic nuclei as a function of nucleon numbers.

[1] D. Savran, T. Aumann, and A. Zilges, Prog. Part. Nucl. Phys. **70**, 210 (2013).

[2] M. Scheck *et al.*, Phys. Rev. C **87**, 051304(R) (2013).

[3] K. Heyde, P. von Neumann Cosel, and A. Richter, Rev. Mod. Phys. **82**, 2365 (2010).

[4] T. Shizuma *et al.*, Phys. Rev. C **87**, 024301 (2013).

[5] P.-G. Reinhard and W. Nazarewicz, Phys. Rev. C **81**, 051303 (2010).

[6] J. Piekarewicz, Phys. Rev. C **83**, 034319 (2011).

[7] P.-G. Reinhard and W. Nazarewicz, Phys. Rev. C **87**, 014324 (2013).

[8] N. Paar, D. Vretenar, E. Khan, and G. Colo, Rep. Prog. Phys. **70**, 691 (2007).

[9] N. Ryezayeva *et al.*, Phys. Rev. Lett. **89**, 272502 (2002).

[10] A. Leistenschneider *et al.*, Phys. Rev. Lett. **86**, 5442 (2001).

[11] E. Tryggestad *et al.*, Phys. Rev. C **67**, 064309 (2003).

[12] J. Isaak *et al.*, Phys. Rev. C **83**, 034304 (2011).

[13] T. Hartmann, M. Babilon, S. Kamerdzhiev, E. Litvinova, D. Savran, S. Volz, and A. Zilges, Phys. Rev. Lett. **93**, 192501 (2004).

[14] T. Hartmann, J. Enders, P. Mohr, K. Vogt, S. Volz, and A. Zilges, Phys. Rev. Lett. **85**, 274 (2000).

[15] M. Scheck *et al.*, Phys. Rev. C **88**, 044304 (2013).

[16] F. Bauwens *et al.*, Phys. Rev. C **62**, 024302 (2000).

[17] O. Wieland *et al.*, Phys. Rev. Lett. **102**, 092502 (2009).

[18] K. Govaert *et al.*, Phys. Rev. C **57**, 2229 (1998).

[19] P. Adrich *et al.*, Phys. Rev. Lett. **95**, 132501 (2005).

[20] A. Klimkiewicz *et al.*, Phys. Rev. C **76**, 051603(R) (2007).

[21] J. Endres *et al.*, Phys. Rev. Lett. **105**, 212503 (2010).

[22] B. Özel *et al.*, Nucl. Phys. A **788**, 385 (2007).

[23] T. Chapuran, R. Vodhanel, and M. K. Brussel, Phys. Rev. C **22**, 1420 (1980).

[24] J. Enders *et al.*, Phys. Lett. B **486**, 279 (2000).

[25] J. Enders *et al.*, Nucl. Phys. A **724**, 243 (2003).

[26] N. Pietralla *et al.*, Phys. Lett. B **681**, 134 (2009).

[27] L. Käubler, H. Schnare, R. Schwengner, H. Prade, F. Dönau, P. von Brentano, J. Eberth, J. Enders, A. Fitzler, C. Fransen, M. Grinberg, R.-D. Herzberg, H. Kaiser, P. von Neumann-Cosel, N. Pietralla, A. Richter, G. Rusev, Ch. Stoyanov, and I. Wiedenhöver, Phys. Rev. C **70**, 064307 (2004).

[28] N. Benouaret *et al.*, Phys. Rev. C **79**, 014303 (2009).

[29] R. Schwengner *et al.*, Phys. Rev. C **87**, 024306 (2013).

[30] R.-D. Herzberg *et al.*, Phys. Lett. B **390**, 49 (1997).

[31] N. Pietralla, Z. Berant, V. N. Litvinenko, S. Hartman, F. F. Mikhaikov, I. V. Pinayev, G. Swift, M. W. Ahmed, J. H. Kelley, S. O. Nelson, R. Prior, K. Sabourov, A. P. Tonchev, and H. R. Weller, Phys. Rev. Lett. **88**, 012502 (2001).

[32] S. Volz *et al.*, Nucl. Phys. A **779**, 1 (2006).

[33] D. Savran *et al.*, Phys. Rev. Lett. **100**, 232501 (2008).

[34] A. P. Tonchev *et al.*, Phys. Rev. Lett. **104**, 072501 (2010).

[35] N. Kumagai *et al.*, Nucl. Phys. A **329**, 205 (1979).

[36] U. E. P. Berg *et al.*, Phys. Lett. B **103**, 301 (1981).

[37] J. Enders *et al.*, Nucl. Phys. A **636**, 139 (1998).

[38] H. Kaiser *et al.*, Nucl. Phys. A **660**, 41 (1999); **669**, 368(E) (2000).

[39] G. Co', V. De Donno, M. Anguiano, and A. M. Lallena, Phys. Rev. C **87**, 034305 (2013).

[40] P. Papakonstantinou *et al.*, Phys. Lett. B **709**, 270 (2012).

[41] U. Kneissl, H. H. Pitz, and A. Zilges, Prog. Part. Nucl. Phys. **37**, 349 (1996).

[42] U. Kneissl, N. Pietralla, and A. Zilges, J. Phys. G **32**, R217 (2006).

[43] F. R. Metzger, Prog. Nucl. Phys. **7**, 54 (1959).

[44] D. Rück, Diploma thesis, Insititut für Kernphysik, Giessen, 1982 (unpublished).

[45] J. Enders *et al.*, Eur. Phys. J. A **31**, 15 (2007).

[46] A. Richter, in *EPAC 96: Proceedings of the Fifth European Particle Accelerator Conference* (Institute of Physics, Bristol, Philadelphia, 1996), p. 110.

[47] P. Mohr *et al.*, Nucl. Instrum. Methods Phys. Res., Sect. A **423**, 480 (1999).

[48] S. Agostinelli *et al.*, Nucl. Instrum. Methods Phys. Res., Sect. A **506**, 250 (2003).

[49] D. I. Sober *et al.*, Phys. Rev. C **31**, 2054 (1985).

[50] H. Junde, H. Su, and M. A. Chunhui, Nucl. Data Sheets **108**, 773 (2007).

[51] A. A. Katsanos and J. R. Huizenga, Phys. Rev. **159**, 931 (1967).

[52] M. A. Basher, H. R. Siddique, A. Husain, A. K. Basak, and H. M. Sen Gupta, Phys. Rev. C **45**, 1575 (1992).

[53] H. R. Prabhakara *et al.*, J. Phys. G: Nucl. Part. Phys. **4**, 1101 (1978).

[54] V. G. Soloviev, *Theory of Atomic Nuclei, Quasiparticles, and Phonons* (Institute of Physics, London, 1992).

[55] P. von Neumann-Cosel *et al.*, Phys. Lett. B **443**, 1 (1998).

[56] K. Langanke, G. Martínez-Pinedo, P. von Neumann-Cosel, and A. Richter, Phys. Rev. Lett. **93**, 202501 (2004).

[57] W. Greiner and J. A. Maruhn, *Nuclear Models* (Springer, Berlin, 1996).

[58] W. Steffen *et al.*, Nucl. Phys. A **404**, 413 (1983).